

Energy Transfer and Connectivity in Chloroplasts: Competition between Trapping and Annihilation in Pulsed Fluorescence Induction Experiments

L. Valkunas,[†] V. Cervinskas,[†] and F. van Mourik^{*,‡}

Institute of Physics, A. Gostauto 12, Vilnius, 2600, Lithuania, and Department of Biophysics, The Free University of Amsterdam, De Boelelaan 1081, 1081 HV Amsterdam, The Netherlands

Received: February 21, 1997; In Final Form: May 5, 1997[⊗]

Despite the fact that fluorescence induction is a very complicated process, the technique is used to obtain information regarding connectivity in photosynthetic systems. The models generally used for the analysis are oversimplified, which in some cases has led to questionable interpretations. Here we describe the effects of nonlinear loss processes in (pulsed) induction experiments and how they obscure the features attributed to large-scale connectivity in chloroplasts. We simulate the fluorescence induction process for finite size domains (1–4 reaction centers per domain) and describe both the trapping process and the generation of triplets by a discrete state model. From our numerical calculations it is demonstrated that singlet–triplet annihilation is unavoidable when using microsecond pulses for actinic illumination.

Introduction

The well-organized cooperation of light-harvesting antennae (LHA) and photochemical reaction centers (RC's) is a key factor for the high (quantum) efficiency of bacterial and plant photosynthetic systems.^{1,2} The recent structural data of light-harvesting complexes in bacteria^{3,4} and plant, i.e., photosystem I (PSI)⁵ and photosystem II (PSII),^{6,7} exposes the light-harvesting apparatus as a well-organized structure. However, the connectivity of the LHA extends far beyond the level of the complexes that can now be visualized from the crystal structures. In the fully assembled photosynthetic apparatus excitations can migrate over domains that are at least 10 times larger, and this level of organization can be probed by spectroscopic methods only. For instance, the fluorescence from the LHA depends on the state of the RC's, in a nonlinear way, which is generally ascribed to large-scale connectivity.^{8–11} The fluorescence yield dependence on the excitation light fluence has been widely used for investigating the connectivity between PS II on millisecond to second time scales,^{1,9–13} as well as on shorter time scales.^{14–16} It is evident that the fluorescence yield is low (F_0) when all reaction centers are in their active/open state, and the fluorescence yield is maximal (F_{\max}) when all RC's are closed, while by increasing the excitation fluence (thereby closing RC's) the fluorescence rises in a nonlinear way, depending on the relative amount of closed RC's. This nonlinear fluorescence induction is due to the connectivity between the PSU's; i.e., in the intermediate situation when only a part of RC's are in the closed state, the exciton can freely migrate through the domain of a common LHA from the RC that is in a closed state to another active RC where it can be very efficiently trapped. It is known that in the case of totally disconnected PSU's (the puddle model) the shape of the fluorescence induction on the excitation fluence is exponential,¹³ and in the case of connected PSU's (the lake model) this shape is sigmoidal.¹³ In the lake model the main parameter (p) of the theory is determined by the ratio of the excitation trapping rates by open and closed RC's, and this parameter fully defines the shape of the induction curve and the ratio $R = F_{\max}/F_0$. The induction experiment therefore is

not very sensitive for the diffusion radius of the excited states; in the lake model trapping is always trap limited. Therefore the “size” of the antenna can only be obtained from annihilation measurements.^{17–21} Quenching by triplet states is generally much more efficient than by open RC's, both in photosynthetic bacteria^{21,22} and in chloroplasts,^{23,24} and is therefore close to migration limited. When modeling fluorescence induction and S–T annihilation simultaneously, finite antenna sizes have to be taken into account. Moreover, by using this approach, the effects of singlet–triplet annihilation in the presence of heterogeneity in the domain size (α and β centers^{25,26}) can also be evaluated. As we will show, singlet–triplet annihilation has a more pronounced effect in larger domains. Therefore, in a mixed system where both small and large (more than one connected RC) domains occur, singlet–triplet annihilation will be most pronounced in the larger domains. Since these large domains are responsible for the sigmoidal character of the induction curves, the sigmoidicity in a mixed system is easily lost.

In this paper we discuss the competition between trapping and annihilation processes in chloroplasts and, more specifically, the effects of singlet–triplet annihilation on fluorescence induction experiments when using short actinic flashes. The excited state dynamics of chloroplasts from higher plants is much more complicated than that of simple photosynthetic bacteria. Even when using powerful time-resolved fluorescence techniques, it is very hard to disentangle all the kinetic components²⁵ and to attribute them to the underlying photo-physical phenomena. The presence of two photosystems and the heterogeneity of PS2 are responsible for this.²⁷ Of course, the situation is even more complicated once nonlinear techniques are applied like fluorescence induction. Nevertheless, fluorescence induction is a popular technique that easily gives information of the overall functioning of the photosynthetic apparatus. The shape of the induction curves of photosynthetic bacteria⁸ and chloroplasts^{9,24} is generally believed to reflect the connectivity between reaction centers. In chloroplasts it was observed that the shape of the induction curve depends on the length of the actinic light flash.^{13,15} This phenomenon was successfully explained by a two-hit model^{12,13} for the closing of the RC's. However, the lifetime ($\sim 1–10 \mu\text{s}$) associated with the intermediate state has not been observed in time-resolved

^{*}To whom correspondence should be addressed.

[†]Institute of Physics.

[‡]The Free University of Amsterdam.

[⊗] Abstract published in *Advance ACS Abstracts*, August 15, 1997.

experiments. More recently, singlet–triplet annihilation was proposed as an alternative explanation for the pulse length effect.²⁸ In this case the intermediate lifetime is the lifetime of the carotenoid triplets. The quenching of antenna excitations by carotenoid triplets has been studied in photosynthetic bacteria and chloroplasts.²⁹ Due to the more simple architecture of the photosynthetic apparatus of the purple bacteria, also the competition among singlet–singlet annihilation,²⁰ quenching by triplets,^{21,22} and fluorescence induction is well documented. Here we investigate under what conditions (singlet–triplet) annihilation can compete with trapping by reaction centers in chloroplasts.

Annihilation experiments performed with picosecond pulses in purple bacteria are a clear example where (singlet–singlet) annihilation fully prohibits trapping by RC's. When using 35 ps pulses, no induction is observed despite the only slightly longer (compared to the pulse duration) trapping time of ~ 50 ps.²⁰

An intermediate situation occurs when pulses much longer than the excited state lifetime (trapping time) are used; in this case S–S annihilation is less important, but triplet states accumulated during the pulse can act as quenchers.^{21–23} The parameters that now rule the competition are the quantum yield of triplet formation and the efficiency of the quencher. For purple bacteria it was found that triplet states are about 5 times more efficient as quenchers than open RC's.²¹ Therefore, despite the relatively low yield of triplets ($< 5\%$ with open RC's), annihilation and trapping were found to be of comparable magnitude when using 5 ns pulses with *Rhodospirillum rubrum* chromatophores.²²

So what is the situation in chloroplasts? Here the number of antenna pigments per RC is about an order of magnitude higher than in *Rs. rubrum*, and so is the trapping time. When using (sub)microsecond pulses, the most important process is clearly S–T annihilation²³ by carotenoid triplets (car^T). These car^T have a lifetime of $\sim 6 \mu\text{s}$, and the intersystem crossing rate in chloroplasts was²³ estimated to be $1.4 \times 10^8 \text{ s}^{-1}$. At high pulse energies fluorescence yields reduced by a factor of > 10 (compared to chloroplasts with closed RC's) were observed at concentrations of $\sim 2 \text{ car}^T$ per RC; i.e., car^T are at least 3 times more “efficient” quenchers than open RC's (presuming $R = 4$).

In the following we first explore under which conditions singlet–triplet annihilation processes will perturb a two-pulse fluorescence induction experiment so as to change the shape of the curve. In the second section we will also calculate the effect of singlet–triplet annihilation on the apparent value of R , since this is a quantity that can be obtained more easily from an experiment.

Methods

Let us consider domains that contain m RC's which are quenchers for excitons in a common LHA. Also triplets, which act as very efficient quenchers of excitons, are taken into account. The case when only one of these two exciton quenching channels is active has already been considered.¹⁸ It is evident that when RC's are the only exciton quenchers, the fluorescence rises from its minimal value F_0 , when all RC's are open, to the maximal value F_{max} , when all RC's are closed, while in the case if triplets are the only quenchers, an opposite situation takes place because the generation of the triplets diminishes the fluorescence quantum yield and, moreover, triplets once present in a domain reduce the probability of the creation of additional triplets. In the first case the fluorescence induction saturates when all RC's becomes closed while in the

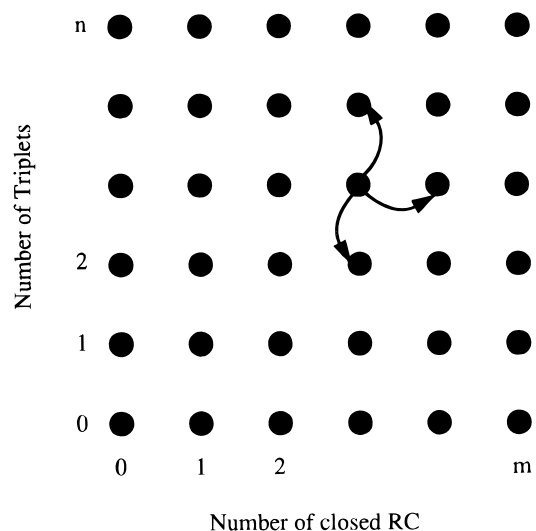


Figure 1. Scheme of the states of a domain characterized by the number of open and closed RC, and the number of triplet states, with the corresponding transitions between these states. Within the time window of the calculations (and the experiments) the closing of RC's is irreversible.

second case no saturation of the carotenoid triplets can be achieved because of the already existing triplets. The case when both these quenching channels are active in an infinitely large domain (the lake model) recently has been considered.²⁸ Here we will consider the finite size domains containing m RC's that are connected via a common LHA, which is a more appropriate treatment of S–T annihilation since this process is possibly close to migration limited.

In this case the state of the system can be characterized by a number of closed and/or open RC's and the number of triplets that are present at a given moment in the course of the excitation lifetime. Let us define i as the number of open RC's in the domain ($0 \leq i \leq m$) and T ($0 \leq T \leq n$) as the number of triplets in the domain. The state of the system changes when an exciton is trapped by an open RC or when a triplet state is formed. Thus, the processes can be represented by transition between quantum states of the domain determined by different numbers of i and T as shown in Figure 1. The vertical transitions in Figure 1 correspond to the formation/decay of a triplet state. The horizontal transitions correspond to the closing of an RC. Here we do not take into account the fact that the RC can return to the open state, which is correct for transition times much longer than the mean time of the process under consideration. Of course, the triplets do decay on the time scale of the experiment, and this is crucial for the pulse length effect. We will restrict ourselves to the case of two RC states, i.e., open and closed, and we also presume efficient S–T annihilation which limits the range of the number of triplets per domain that have to be taken into account to less than 4 in all practical cases.

Let us assume that our systems are dark-adapted, i.e., that initially all RC's are in the open states, and no triplets are present in the domain. Then the singlet excitons in the LHA, created by the excitation pulse, stimulate the transition of the RC's into the closed states, and also some generation of triplets will occur. At this point two time scales can be distinguished: one of them involves the lifetime of the singlet excitons which is (at low excitation densities) determined by the trapping rate, i.e., by K_0 for open RC's and by K_c for closed RC's, which are of the order of $10^3 \mu\text{s}^{-1}$; while another is associated with the lifetime of triplets, i.e., $\tau_T \cong 5\text{--}10 \mu\text{s}$. Therefore, values that are related

to quenching by the RC will be normalized to K_0 , and values associated with the triplets will be normalized to τ_T units.

In order to determine the kinetic equations for the amount of singlet $n_{i,T}$ and triplet T excitations in a domain, characterized by i closed RC's, the corresponding rate parameters and the probability $P_{i,T}$ to find such a domain under the selected conditions have to be defined. By using the normalization to K_0 , the overall exciton quenching rate by the open RC's in such a domain can be described by¹⁸

$$K_0^i = 1 - i/m \quad (1)$$

and using the same normalization to K_0 the excitation quenching rate due to the closed RC's equals

$$K_c^i = (1 - p)(i/m) \quad (2)$$

where

$$p = (K_0 - K_c)/K_0 \quad (3)$$

is the value which determines the connectivity of the PSU.^{12,13,18,29}

The relative rates for intersystem crossing $I_T = K_{ic}/K_0$, singlet-triplet quenching $\Gamma = \gamma_{ST}/K_0$, and the triplet lifetime τ_T determine the interplay between the singlet and triplet subsystems. Below we express the pulse lengths and the delay time between the actinic "pump" pulse and the probe pulse and the pulse lengths of the actinic and probe pulses, τ_{ex} and τ_{prob} , in units of α , where $\alpha = \tau_T K_0$ is the parameter that determines the ratio of the two time scales mentioned above. By normalizing the time scale in K_0 units, the corresponding kinetic equations for the amount of singlets in the domain can be defined as follows:

$$\frac{dn_{i,F}}{dt} = J - \left(1 - p \frac{i}{m}\right)n_{i,T} - I_T n_{i,T} - \frac{\Gamma}{m} T n_{i,T} \quad (4)$$

where J is the excitation fluence (the pulse width is also normalized to the time scale K_0). Here the rate of singlet triplet annihilation Γ is divided by the domain size to account for different domain sizes in the simulations. This approach is correct for domains smaller than the diffusion radius of the singlet excitations.

We will consider the fluorescence induction on a microsecond time scale; thus, in eq 4 the kinetics determined on the time scale of the singlet exciton lifetime can be considered to be steady state, giving

$$n_{i,T} = \frac{J}{1 - p \frac{i}{m} + I_T + \frac{\Gamma T}{m}} \quad (5)$$

The kinetic equations for the probabilities $P_{i,T}$ (time scale in K_0 units) are related to the following recurrence relations:

$$\frac{dP_{i,T}}{dt} = \mu(K_0^{i-1} n_{i-1,T} P_{i-1,T} - K_0^i n_{i,T} P_{i,T}) + I_T (n_{i,T-1} P_{i,T-1} - n_{i,T} P_{i,T}) + \frac{1}{\alpha} ((T+1) P_{i,T+1} - T P_{i,T}) \quad (6)$$

where $0 \leq i \leq m$, and μ is the quantum yield of trapping by the RC.

Equations 5 and 6 can be used for either calculating single-pulse fluorescence induction⁹⁻¹¹ curves or for calculating two-pulse (pump-probe) fluorescence induction^{12,15,16} curves. In the latter case calculations of $n_{i,T}$ and $P_{i,T}$ have to be carried out in three steps: during the pump pulse action (the excitation

fluence J_{ex}), between pulses, and during the probe pulse action (probe fluence $J_{prob} \ll J_{ex}$). Accordingly, the fluorescence induction in the i th state can be determined as follows:

$$F_{i,T} = (K_f/J\tau) \int_{t_0}^{t_0+\tau} n_{i,T}(t') dt' \quad (7)$$

where K_f is the fluorescence rate. In the one-pulse experiment τ corresponds to the pulse length. In the two-pulse (pump-probe) case J corresponds to J_{prob} , and τ is the duration of the probe pulse (t_0 is the start of the probe pulse). Thus, for the steady-state condition (5) it follows that

$$F_{i,T} = K_f n_{i,T} / J \quad (8)$$

and the fluorescence induction F which is observed equals

$$F = \sum_{i=0}^m P_{i,T} F_{i,T} \quad (9)$$

Equations 5 and 6 are solved numerically for each i th state of the system, which contains T triplets. Because $J_{prob} \ll J_{ex}$, the fluorescence quantum yields are obtained as a function of the fluence, $J = J_{ex}$, of the actinic pulse, according to eq 9.

Calculations

The finite number of RC's per domain is the main point of the present work, which makes it different from the case of the infinitely large system ($m \rightarrow \infty$), i.e., from the lake model, which has been considered in a previous paper.²⁸ As has already been shown, the influence of singlet-triplet annihilation in large domains can be observed on the shape of the fluorescence induction curve, even when the fluorescence induction amplitude (R) is hardly changed. A problem with the previous treatment was that simulating the triplet population using the lake model is not appropriate, since the action radius of the triplets, which is determined by the singlet diffusion length, is probably limited by the finite size of a PSU. Because trapping in chloroplasts is trap limited, the actual size of the lake has only limited influence on the induction kinetics. However, for a close to migration-limited annihilation process the size of the lake is of importance. When simulating the annihilation using a lake model, an overestimation of the inhibiting effect of triplets on the formation of more triplets is made. Thus, in large domains the amount of triplets remains small (relative to the amount of RC's), the effects on the induction kinetics quenching by RC's are very gradual, and trapping is competing well with the quenching by triplets.²⁸ However, this would not be the case for finite size domains containing a small number of RC's. Thus, we will consider the limiting case of domains containing a low number of RC's ($m = 1-4$). The other parameters of the system are chosen as follows: According to the previous analysis of the lake model, the sigmoidal shape of the fluorescence induction curve can be distinguished only when the connectivity parameter^{1,9,13,18} p is > 0.5 . Moreover, it has also been shown¹² that the difference between domains containing different numbers of RC's becomes indistinguishable when R is < 4 . Thus, due to the relation between both these values

$$R = 1/(1 - p) \quad (10)$$

which is correct for the lake model,^{1,8,16,19} we have assumed that $p = 0.8$. For this value of the connectivity parameter the calculated fluorescence induction curve is sigmoidal in the case when the singlet-triplet annihilation is not taken into account (Figure 2). The triplet effects are defined by the following

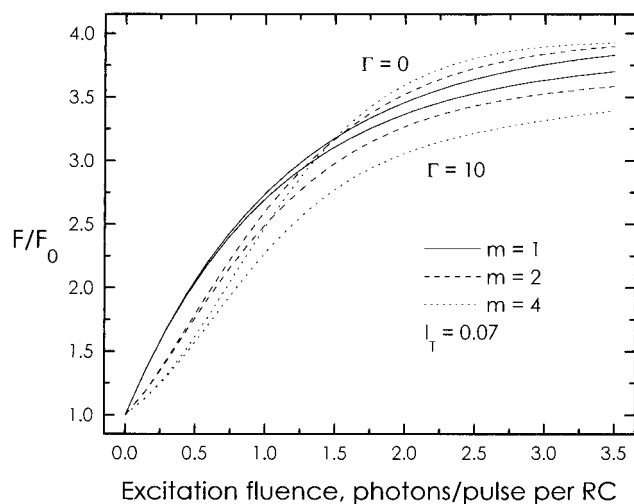


Figure 2. Fluorescence induction curves for an actinic pulse durations $\tau_{\text{ex}} = 0.01\alpha$ ($\alpha = \tau_T K_0$) for two values of Γ , 0, and 10 and different numbers of connected RC's ($m = 1, 2, 4$). The time delay between the actinic pulse and the probe pulse was 10α .

parameters: Γ , which is the singlet–triplet annihilation rate, and I_T , the rate of intersystem crossing. According to eqs 5 and 10, the effect of the last parameter determines a renormalization of the excitation fluence, i.e., $J/(1 + I_T)$, as well as the connectivity parameter, $p/(1 + I_T)$, and the singlet–triplet annihilation rate, $\Gamma/(1 + I_T)$. Therefore, the demands for the presence of a sigmoidal induction curve can now be reformulated as $p/(1 + I_T) > 0.5$, and the effective value of p in these calculations equals 0.75 when the loss due to intersystem crossing is taken into account.

The quantum yield of triplets has been measured³⁰ to be 5–10%. Therefore, in the following we assume I_T to be 0.07, and the effective value of R in these calculations equals 0.75 once the loss due to intersystem crossing is taken into account. The effect of triplets present in the system is then determined by the singlet–triplet annihilation rate Γ , for which we take values between 0 and 10.

It is easy to show that for these parameters the induction curve will be affected by annihilation: at least m excitations are needed in a domain to close all RC's, and with the given triplet yield this implies that in a significant fraction ($>0.07m$) of the domains a triplet state will be formed. Within such a small domain S–T annihilation will severely hamper the closing of the RC's when the pulse length is on the order of the lifetime of the triplet states, since these triplet states can then act as quenchers of subsequent excitations in the domain.

Figure 2 shows the effect of singlet–triplet annihilation for different domain sizes for two values of Γ . Obviously, the effect is larger for the larger domains, and the loss of the sigmoidal shape is clearly visible for the large domains. The sigmoidicity of the curves can be estimated from the tangent of the initial (lowest excitation fluence) part of the curve. These curves were calculated for long waiting times between the actinic and the probe pulse so that all triplet states have disappeared once the probe pulse arrives. Therefore, the probe pulse just probes the closing of the RC's.

In Figure 3 the probe pulse is given just after the actinic pulse, so that the triplet states can also directly quench the fluorescence generated by the probe pulse. In this case even induction ratio's less than 1 can be obtained.¹⁶ In Figure 4 the delay between the actinic and probe pulses is changed, this gives the most easily observed effect of the triplet lifetime on the induction curves. However, the most important time scale in the experiment is the pulse length of the actinic pulse relative to the triplet lifetime.

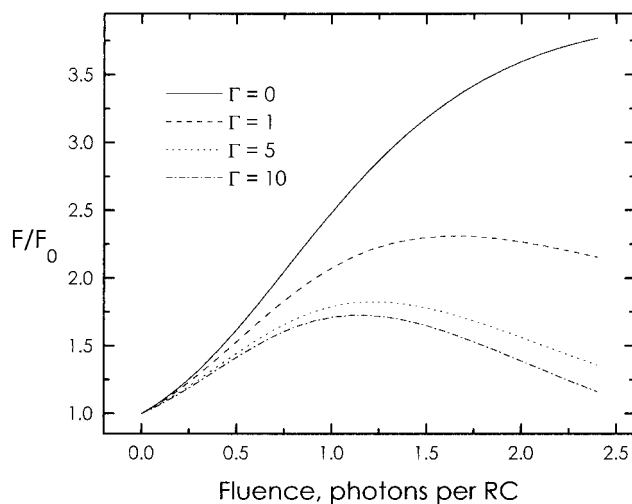


Figure 3. Fluorescence induction curves at the end of the actinic pulse, for an actinic pulse length of 0.2α and for different values of Γ . For all curves $I_T = 0.07$ and $m = 4$.

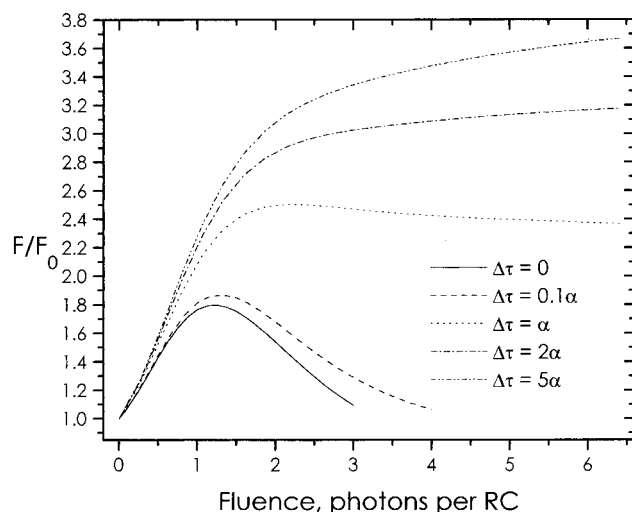


Figure 4. Fluorescence induction curves at different delays between the actinic and probe pulses. For all curves $\tau_{\text{ex}} = \tau_{\text{prob}} = 0.2\alpha$, $I_T = 0.07$, $\Gamma = 10$, and $m = 4$.

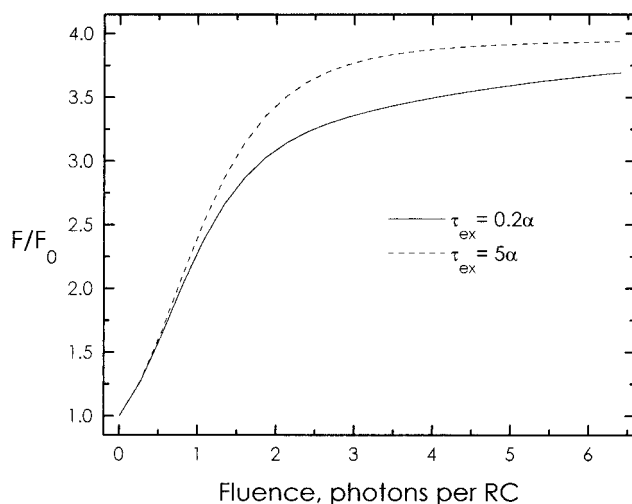


Figure 5. Fluorescence induction curves for two different actinic pulse lengths. The time delay between the actinic pulse and the probe pulse was 10α , $I_T = 0.07$, $\Gamma = 10$, and $m = 4$.

Figure 5 shows the induction curves for two actinic pulse lengths: one much shorter than the triplet lifetime and one much longer than the triplet lifetime. The difference in shape between

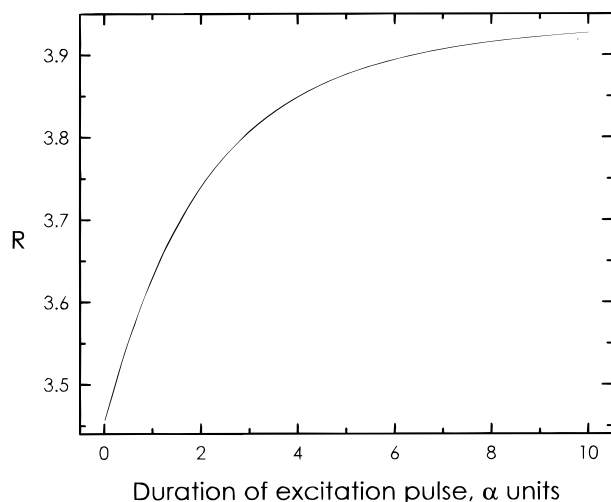


Figure 6. Dependence of the induction ratio, when measured with four excitations per RC, on the duration of the actinic pulse for $m = 4$, $\Gamma = 10$, $I_T = 0.0$; the time delay between the actinic pulse and the probe pulse was 10α .

these two curves is clearly visible, and the change occurs in the pulse length region (5α corresponds to a pulse length of about $50 \mu\text{s}$) where this was actually observed experimentally.^{13,15} The experimental value of R under these conditions is not well-defined since obviously the simulations predict that for very intense actinic pulses all RC's will be closed and the same induction ratio will be obtained ultimately, with or without annihilation. In practice, the R values are always smaller for short pulses, even with very intense actinic pulses, and we have to presume that at some point other nonlinear loss processes, i.e., singlet-singlet annihilation, start to occur. Therefore, we can only define the R value in relation to a finite number of photons per RC. In Figure 6 we have plotted the induction ratio corresponding to four excitations per RC as a function of the pulse length. This ratio is more easily measured experimentally than the shape of the curve and therefore gives more useful information about the pulse length effect.

Concluding Remarks

Here we have explored the dependence of the competition between trapping and S-T annihilation in chloroplasts on the actinic pulse length. Calculations were performed on the basis of the experimentally determined triplet yield in chloroplasts and reasonable estimates for the rate of singlet-triplet annihilation. The value of Γ that we used, we presumed it to be a 10 times more efficient quencher than open RC's, is about a factor of 2 larger than what is generally presumed. However, the interpretation of the experiments depends on the model and more specifically on the actual size of the domains. If, as we presume here, the size of the domains is limiting the migration radius of the excitations, then the experimentally determined value of Γ is an underestimation.

The calculations clearly demonstrate that when using microsecond flashes to cause fluorescence induction, singlet-triplet annihilation will perturb the induction curve. This effect is a more natural explanation for the observations of France et al.¹⁵ than the two-hit model proposed by Valkunas et al.¹³

One aspect that has not been taken into account so far is the

heterogeneity in the domain sizes of PS2. This heterogeneity can enhance the effects observed here, and this can be appreciated already from Figure 2. It is generally assumed that two types of PS2 domains occur in chloroplasts, the so-called α and β centers. The β centers are small domains ($m = 1$), and they give rise to exponential induction curves. The α centers are the ones that are responsible for the sigmoidal character of the induction curves. The observed induction curves are the average of the two types. Due to their larger size, the induction kinetics of the α centers ($m > 4$) are more affected by S-T annihilation, and this enhances the overall change in shape of the induction curves.

Acknowledgment. This work was supported (for L.V. and V.C.) by Joint Grant ISF-Lithuanian Government No. LH6100.

References and Notes

- (1) Dau, H. *Photochem. Photobiol.* **1994**, *60*, 1-23.
- (2) van Grondelle, R.; Dekker, J. P.; Gillbro, T.; Sundström, V. *Biochim. Biophys. Acta* **1994**, *1187*, 1-65.
- (3) McDermott, G.; Prince, S. H.; Freer, A. A.; Hawthornthwaite-Lawless, A. M.; Papiz, M. Z.; Cogdell, R. J.; Isaacs, N. W. *Nature* **1995**, *374*, 517.
- (4) Karrasch, S.; Bullough, P. A.; Ghosh, R. *EMBO J.* **1995**, *14*, 631.
- (5) Schubert, W. D.; Klukas, O.; Krau, N.; Saenger, W.; Fromme, P.; Witt, H. T. In *Photosynthesis: from Light to Biosphere*; Mathis, P., Ed.; Kluwer Academic Publishers: Dordrecht, The Netherlands, 1995; Vol. 2, pp 3-10.
- (6) Kühlbrandt, W.; Wang, D. N.; Fujiyoshi, Y. *Nature* **1994**, *367*, 614-621.
- (7) Boekema, E. J.; Hankamer, B.; Blad, D.; Kruip, J.; Nield, J.; Boonstra, A. F.; Barber, J.; Rögner, M. *Proc. Nat. Acad. Sci. U.S.A.* **1995**, *92*, 175-179.
- (8) Vredenberg, W. J.; Duysens, L. N. M. *Nature* **1963**, *197*, 355-357.
- (9) Joliot, A.; Joliot, P. *C. R. Acad. Sci. Paris* **1964**, *258*, 4622-4625.
- (10) Lavorel, J.; Joliot, P. *Biophys. J.* **1972**, *12*, 815-831.
- (11) Joliot, P.; Joliot, A. *Biochim. Biophys. Acta*, **1977**, *462*, 559-574.
- (12) Valkunas, L.; Geacintov, N. E.; France, L.; Breton, J. *Biophys. J.* **1991**, *59*, 397-408.
- (13) Valkunas, L.; Geacintov, N. E.; France, L. L. *J. Luminesc.* **1992**, *51*, 67-78.
- (14) Deprez, J.; Dobek, A.; Geacintov, N. E.; Paillotin, G.; Breton, J. *Biochim. Biophys. Acta* **1983**, *725*, 444-454.
- (15) France, L. L.; Geacintov, N. E.; Breton, J.; Valkunas, L. *Biochim. Biophys. Acta* **1992**, *1101*, 105-119.
- (16) France, L. L. Ph.D. Thesis, New York University, New York, 1989.
- (17) van Grondelle, R. *Biochim. Biophys. Acta* **1985**, *811*, 147-195.
- (18) Paillotin, G.; Geacintov, N. E.; Breton, J. *Biophys. J.* **1983**, *44*, 65-77.
- (19) Valkunas, L.; Liuolia, V.; Freiberg, A. *Photosynth. Res.* **1991**, *27*, 83-95.
- (20) Deinum, G.; Aartsma, T. J.; van Grondelle, R.; Amesz, J. *Biochim. Biophys. Acta* **1989**, *976*, 63-69.
- (21) Monger, T. G.; Parson, W. W. *Biochim. Biophys. Acta* **1977**, *460*, 393-407.
- (22) van Mourik, F.; Visscher, K. J.; Mulder, J. M.; van Grondelle, R. *Photochem. Photobiol.* **1993**, *57*, 19-23.
- (23) Breton, J.; Geacintov, N. E.; Swenberg, C. S. *Biochim. Biophys. Acta* **1979**, *548*, 616-635.
- (24) Kolubayev, T.; Geacintov, N. E.; Paillotin, G.; Breton, J. *Biochim. Biophys. Acta* **1985**, *808*, 66-76.
- (25) Roelofs, T. A.; Holzwarth, A. R. *Biophys. J.* **1992**, *61*, 1147-1163.
- (26) Melis, A.; Homann, P. H. *Photochem. Photobiol.* **1976**, *23*, 343-350.
- (27) Govindjee *Photosynth. Res.* **1990**, *25*, 151-160.
- (28) Cervinskis, V.; Valkunas, L.; van Mourik, F. *Lith. J. Phys.* **1994**, *34*, 375-378.
- (29) Breton, J.; Geacintov, N. E. *Biochim. Biophys. Acta* **1980**, *594*, 1-32.
- (30) Kramer, H.; Mathies, P. *Biochim. Biophys. Acta* **1980**, *593*, 319-329.